

PACS numbers: 42.30.Wb; 42.25.Gy; 42.25.Hz
DOI: 10.1070/QE2014v044n07ABEH015465

Achromatic registration of quadrature components of the optical spectrum in spectral domain optical coherence tomography

P.A. Shilyagin, G.V. Gelikonov, V.M. Gelikonov, A.A. Moiseev, D.A. Terpelov

Abstract. **We have thoroughly investigated the method of simultaneous reception of spectral components with the achromatised quadrature phase shift between two portions of a reference wave, designed for the effective suppression of the 'mirror' artefact in the resulting image obtained by means of spectral domain optical coherence tomography (SD OCT). We have developed and experimentally tested a phase-shifting element consisting of a beam divider, which splits the reference optical beam into the two beams, and of delay lines being individual for each beam, which create a mutual phase difference of $\pi/2$ in the double pass of the reference beam. The phase shift achromatism over a wide spectral range is achieved by using in the delay lines the individual elements with different dispersion characteristics. The ranges of admissible adjustment parameters of the achromatised delay line are estimated for exact and inexact conformity of the geometric characteristics of its components to those calculated. A possibility of simultaneous recording of the close-to-quadrature spectral components with a single linear photodetector element is experimentally confirmed. The suppression of the artefact mirror peak in the OCT-signal by an additional 9 dB relative to the level of its suppression is experimentally achieved when the air delay line is used. Two-dimensional images of the surface positioned at an angle to the axis of the probe beam are obtained with the correction of the 'mirror' artefact while maintaining the dynamic range of the image.**

Keywords: *optical coherence tomography, autocorrelation artefacts, complex amplitude of the optical spectrum.*

1. Introduction

The method of optical coherence tomography (OCT), as a technique to visualise the internal scattering structure of optically turbid media using low-coherent radiation, was proposed in [1, 2]. With the development of the element base and computer technology, the originally proposed correlation methods [3], which perform direct measurements of the amplitudes of the interference signal and the reference wave scattered from a certain depth determined by the position of the reference radiation reflector, were replaced by spectral methods capable of recording the optical spectrum of the interference signal, whilst the information about the spatial distribution of the scatterers in the object under study is reconstructed using mathematical transformations [4, 5].

The use of spectral methods allows high speed OCT-images to be obtained [6]; however, the spectral domain method for recording the interference signal and its digitising may represent a source of a number of features and artefacts that arise in the OCT-image. Thus, the spectral sensitivity of OCT depends significantly on the path difference between the reference and scattered waves. Due to a finite size of the image of the individual spectral component on the photodetector plane, limited coherence length of that component [7], discretisation of spectral counts and possible interactions between the individual photodetectors, the signal decreases with increasing path difference between the reference and scattered waves. Such a decrease in sensitivity can be minimised by placing the reference plane in the depth of the object, albeit the classic implementation of the spectral method provides only recording the real spectra of the interfering waves, making it impossible to determine the sign of the delay, and hence the scatterer location relative to the reference plane. In other words, due to the peculiarities of the Fourier transform, the reconstructed image turns out symmetrical relative to the zero path difference and the additional elements ('mirror' artefacts) arise in the work region of the object space on the other side of the reference plane [8–13].

To solve this problem, a number of algorithms have been proposed to allow for separate observation of the interfering component with positive and negative mutual delays, namely, the method of complex OCT. The common element of such an algorithmic technique is the multiple recording of the sum of the interfering waves with a different mutual delay [8, 11, 12, 14]. This allows determination of the complex spectral amplitude of the sum of the interfering waves, thereby removing the degeneracy of the reconstructed image in the sign of the delay between the reference and scattered waves, which is inherent in the spectral method. From the user's standpoint, this doubles the effective visualisation of the object's depth structure and reduces the losses of the useful signal, associated with the contrast deterioration when recording a highly 'jagged' spectrum by means of the photodetector elements of finite width. Currently, in most cases, the delay between the reference and object waves is varied by changing the optical path length of the reference arm. This causes the appearance of an additional phase delay for the spectral components different from the central one, for which a required delay is set. The result is a disturbance of the phase relationships between the individual components, which in

P.A. Shilyagin, G.V. Gelikonov, V.M. Gelikonov, A.A. Moiseev Institute of Applied Physics, Russian Academy of Sciences, ul. Ul'yanova 46, 603950 Nizhnii Novgorod, Russia; Nizhnii Novgorod State Medical Academy, pl. Minina i Pozharskogo 10/1, 603005 Nizhnii Novgorod, Russia; e-mail: paulo-s@mail.ru;
D.A. Terpelov Institute of Applied Physics, Russian Academy of Sciences, ul. Ul'yanova 46, 603950 Nizhnii Novgorod, Russia

Received 10 March 2014; revision received 15 May 2014
Kvantovaya Elektronika **44** (7) 664–669 (2014)
Translated by M.A. Monastyrskiy

turn substantially restricts the applicability of the method when using the broadband sources [15, 16]. Despite the fact that there exists a known approach to ensure the achromatic phase shift between the different parts of the radiation using the multi-port fibre couplers [17], this method is not used in the schemes with parallel recording of spectral components.

A method to form an achromatised phase shift was first described by us in [18]; however, the problem of the stability of the method with respect to possible deviations of the physical parameters of the individual elements that form a phase-shifting element has not yet been considered. The efficiency of the method in comparison with the method that uses the air line delay also has not been confirmed experimentally.

2. Determining the stability of the achromatised phase shift formation

The method of forming the achromatic phase shift consists in the use of the composite delay line in the reference beam to separate the latter into two equal parts (Fig. 1). The components of the line have different optical thickness which, in the double-pass regime, results in a phase difference of $\pi/2$ between the portions of the reference beam. The difference of the dispersion characteristics of the components allows a high degree of achromatism to be attained in the phase shift within the detected radiation spectrum.

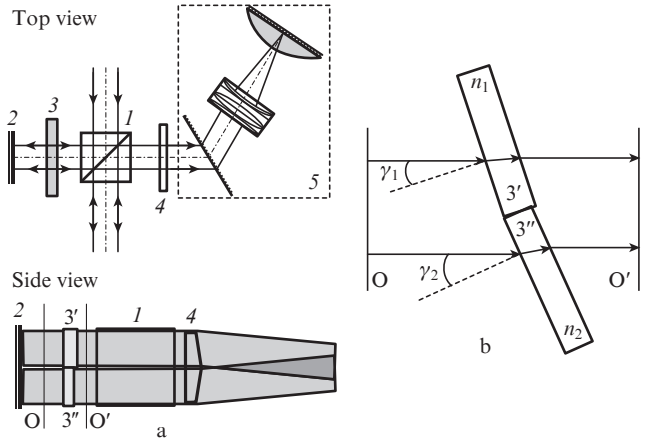

Figure 1. (a) Principal optical scheme of the recording block for a SD OCT with a composite delay line and (b) a variant of implementation of the delay line components in the form of plates placed at an angle to the optical axis of the beam: (*1*) beam splitter; (*2*) reference reflector; (*3*), (*3′*) and (*3′′*) elements of the phase-shifting unit; (*4*) beam divider; (*5*) spectrometer.

When using the elements representing the plane-parallel plates of optical materials with different dependences of the refractive index $n_1(\omega)$ and $n_2(\omega)$ on the optical frequency, as well as different thicknesses h_1 and h_2, the difference in the phase shift acquired by each of the frequency components of the optical radiation incident normally to the surface of the element after its passing through the elements is given by

$$\Delta\varphi(\omega) = \frac{\omega}{c}\{[n_1(\omega) - 1]h_1 - [n_2(\omega) - 1]h_2\}. \quad (1)$$

It is easy to see that, given the dispersion characteristics of the material [the refractive indices $n_1(\omega)$ and $n_2(\omega)$] and a fixed thickness of one of the elements, condition (1) uniquely determines the thickness of the other element at which the difference between the phase shifts of the radiation components with the optical frequency ω is equal to $\Delta\varphi$. This allows the imposition of the condition $\Delta\varphi$ = const for two optical spectrum frequencies ω_1 and ω_2:

$$\begin{aligned} \frac{\omega_1}{c}\{[n_1(\omega_1) - 1]h_1 - [n_2(\omega_1) - 1]h_2\} &= \frac{\pi}{4}, \\ \frac{\omega_2}{c}\{[n_1(\omega_2) - 1]h_1 - [n_2(\omega_2) - 1]h_2\} &= \frac{\pi}{4}. \end{aligned} \quad (2)$$

Obviously, the system of linear equations (2) has a unique solution if the ratio of the Abbe coefficients of both materials is not a constant within the frequency range used. However, a number of difficulties arise when manufacturing the phase shifter elements from different optical materials. The main difficulty is not high enough reproducibility of characteristics of optical glass, which may vary between batches. Despite the relative smallness of such deviations, they can lead to inoperability of the system described. Another difficulty is the complexity of production of thin glass plates, because for most of the available pairs of glass the calculated thickness of plates amounts to units – tens of micrometres, while the accuracy with which the thickness of the plates must withstand should be circa 1/8 of the wavelength of the radiation being analysed.

To overcome these difficulties, it was proposed to produce the plates of the same material; herewith, the difference in effective dispersion of the characteristics is ensured by the different tilts of the plates to the axis of the optical radiation propagation, as shown in Fig. 1b. Indeed, in this case the difference in the phase shifts acquired by each frequency component of the incident optical radiation in the plane O′ amounts to [18]

$$\Delta\varphi(\omega) = \frac{\omega}{c}\{[\tilde{n}_1(\omega) - 1]h_1 - [\tilde{n}_2(\omega) - 1]h_2\}, \quad (3)$$

where the effective refractive indices $\tilde{n}_{1,2}$ are determined by the expression

$$\tilde{n}_{1,2}(\omega) = \frac{1}{\sqrt{1 - (\sin^2\gamma_{1,2})/n^2(\omega)}} \times \left\{n(\omega) - \cos\left[\gamma_{1,2} - \arcsin\frac{\sin\gamma_{1,2}}{n(\omega)}\right]\right\} + 1. \quad (4)$$

Herewith, when using the phase-shifting element proposed, the deviation of the phase shift $\Delta\varphi(\omega)$ from a required value φ_0 has a parabolic dependence on the optical frequency, while the phase deviation of the individual spectral components from the required value is up to 100 times lower than within the entire spectral range, unlike the case of using the air delay line similar to that first proposed in [19].

The key point in the analysis of the proposed method for obtaining the achromatic phase shift is to define a criterion, in the frame of which the phase shift between the two parts of the reference beam can be considered as achromatic.

The presence of the mirror artefacts in the images derived by means of the complex version of the method of SD OCT is due to the insufficient orthogonality of the spectral components different from the central one [16]. When using the air delay line, the phase deviation of individual spectral component from a required value is proportional to the difference $\omega - \omega_c$ between its frequency and the centre frequency of the optical spectrum, for which the phase shift is assumed to be exactly established. For the typical values of the width and centre frequency of the spectrum used in the SD OCT, the

phase deviation from the required value at the extreme points of the frequency range is usually less than 10%. This allows us to consider the artefact signal as an additive signal, the spectral amplitude of which is determined by the difference $\Delta\varphi(\omega) - \varphi_0 = \varphi(\omega)$. It can be shown that, for small phase deviations, the artefact signal is determined by the convolution of the Fourier transform of the dependence $\varphi(\omega)$ and the useful signal that is restored using the classical approach of the SD OCT (symmetric with respect to zero path difference).

For a single scatterer, the artefact signal value can be defined as the maximum of the zero and first elements of the Fourier transform of the dependence $\varphi(\omega)$ [the need to consider the first element is due to the fact that the zero element may vanish, which occurs if the integral of $\varphi(\omega)$ taken over the entire interval of its definition is zero]. In general case, for the light sources used in the SD OCT, we can restrict ourselves by the quadratic expansion of $\varphi(\omega)$ with respect to the small parameter $\zeta = (\omega - \omega_c)/\omega_c$:

$$\varphi(\omega) = \varphi_0 + \varphi_1\zeta + \varphi_2\zeta^2, \tag{5}$$

where φ_0, φ_1, and φ_2 are the constants. The value of the zero element of the Fourier transform is defined as

$$f_0 = \left(\varphi_0 + \frac{1}{3}\delta\varphi_2\right)\Delta\omega, \tag{6}$$

where $\delta\varphi_2$ is the range of the dependence $\varphi_2\zeta^2(\omega)$ within the definition range of $[-\Delta\omega/2; \Delta\omega/2]$. The modulus of the first element of the Fourier transform of the dependence $\varphi(\omega)$ appears as

$$|f_1| = \left| i\delta\varphi_1\frac{1}{2\pi} - \delta\varphi_2\frac{2}{\pi^2}\right|\Delta\omega, \tag{7}$$

where $\delta\varphi_1$ is the range of the dependence $\varphi_1\zeta(\omega)$ in the interval of definition. In the case of the air delay line, the factor φ_2 in expansion (5) is strictly zero, while using the achromatised element we have $\delta\varphi_1 \gg \delta\varphi_2$ [18], which allows us to rewrite (7) in the form

$$|f_1| = \delta\varphi_1\Delta\omega/2\pi. \tag{8}$$

It is advisable to define the efficiency of the suppression of the mirror artefact component of the OCT-signal as the ratio of the amplitudes of the components when using the perfectly adjusted air and achromatized delay lines. The efficiency evaluation value that takes into account the first and zero elements of the Fourier expansion can be obtained by the formula

$$\eta = \frac{\Delta\Phi}{\delta\varphi + 2\pi\Delta\varphi(\omega_c)}, \tag{9}$$

where $\Delta\Phi$ is the range of the dependence $\varphi(\omega)$ in case of the air delay line; $\delta\varphi$ is the range of the dependence $\varphi(\omega)$ for the achromatised delay line; and $\Delta\varphi(\omega_c)$ is the phase deviation of the central spectral component at the frequency ω_c from the required value.

Despite the fact that the possibility of attaining the efficiency correction of the delay line dispersion η close to 100 has been predicted in [18], this is hardly possible to implement experimentally because a too high-precision adjustment of the optical circuit is required in that case. At the same time, when using the air delay line in the phase-shifting element at the wavelength and spectral width of the radiation source being typical for OCT, the mirror artefact suppression amounts to ~40 dB (this issue was studied in [16] in more detail), which is comparable to the signal/noise ratio in the real OCT devices (40–50 dB) [16]). For complete elimination of the mirror artefacts, an additional suppression by 10–20 dB is required in most cases, which may be realised even at the dispersion correction efficiency $\eta > 4$ of the delay line (the suppression is greater than 12 dB). For a more complete suppression of the mirror artefact, more stringent criterion $\eta > 12$ can be used, which ensures additional efficiency of the mirror artefact suppression over 20 dB.

Figure 2a shows the profiles of the model signals obtained under the assumption of the use of the air delay line and in the event of a partial compensation of the dispersion using a phase-shifting element in the composite configuration satisfying the criterion $\eta > 4$. The relevant model phase shift distributions are shown in Fig. 2b. The model distribution for the case of a composite delay line is constructed for the BK7 glass plates manufactured for experimental testing (the measured thicknesses of the plates are $h_1 = 610.3$ μm and $h_2 = 672.8$ μm). In the configuration under consideration, the artefact peak suppression using the composite delay is by 11 dB greater compared to introducing the geometrical delay, and amounts

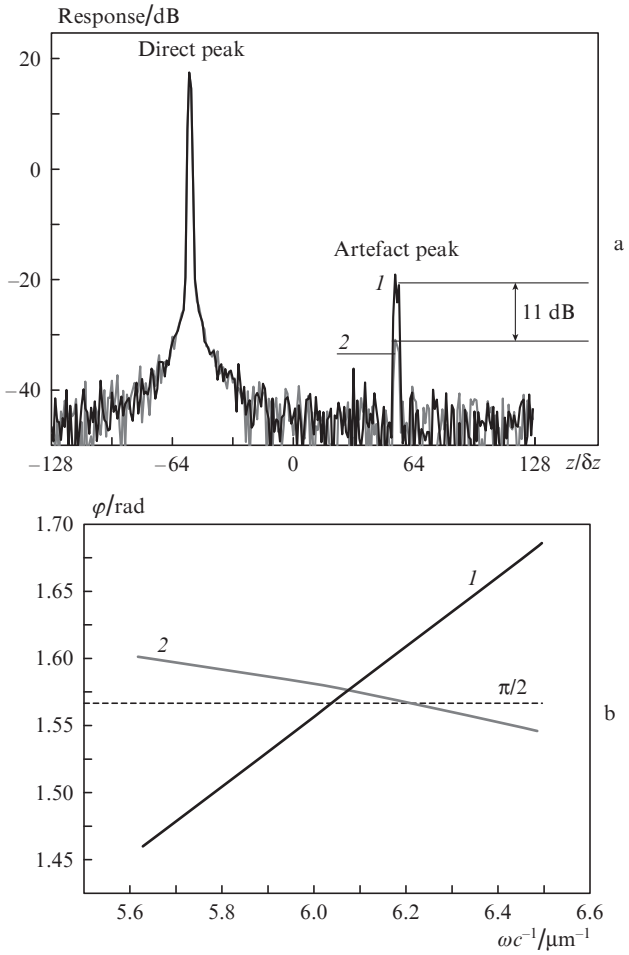

Figure 2. (a) Recovered profiles of the 'scattering' on a mirror placed in the object arm of the interferometer and (b) the phase shift for the model signals using the geometric delay (*1*) and the nonoptimised phase-shifting element matching the criterion $\eta > 4$ (*2*); z is optical delay value, δz is the element of the longitudinal resolution of the system.

to 50 dB relative to the direct peak height. Such a compensation level is, as a rule, sufficient in the studies on biological media to prevent the occurrence of the image artefacts.

The possibility of effective implementation of the technique described to suppress the mirror artefacts in the OCT-images is largely determined by the accuracy of manufacturing of the optical elements of the phase-shifting unit and also by the available accuracy of their mutual arrangement in the experiment. Figure 3 shows the adjustment curve [curve (*1*)] of the composite delay line consisting of BK7 glass plates, the thicknesses of which are found by solving the system of equations (2) for effective refractive indices of the plates (4), which are determined by the angles $\gamma_{1,2}$ of their rotation with respect to the optical axis of the beam:

$$\begin{aligned} &\frac{\omega_1}{c}\{[\tilde{n}_1(\omega_1)-1]h_1-[\tilde{n}_2(\omega_1)-1]h_2\}=\varphi_0,\\ &\frac{\omega_2}{c}\{[\tilde{n}_1(\omega_2)-1]h_1-[\tilde{n}_2(\omega_2)-1]h_2\}=\varphi_0. \end{aligned} \tag{10}$$

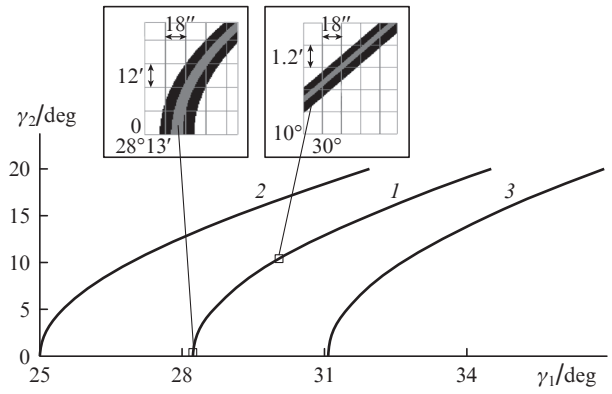

Figure 3. Adjustment curves of the composite delay line at the exact implementation of its components in accordance with the solution of system (10) (*1*), and at deviation of the thickness of one of the components by 11.5 μm in the direction of smaller (*2*) and larger (*3*) values.

Curve (*1*) is plotted for the calculated glass thicknesses h_1 = 610.3 μm and h_2 = 661.3 μm at the rotation angles $\gamma_1 = 0$ and $\gamma_2 = 28.2°$. It is seen that the adjustment of the delay line configuration is available in a wide range of rotation angles of the plates, while the system as whole is less sensitive to the rotation of the thicker plate. The insets in Fig. 3 show the enlarged images of the selected regions of the adjustment curve, in which the composite delay line meets the criteria (8) $\eta > 4$ (black areas) and $\eta > 12$ (grey areas). It is clearly seen that the available range of adjustment angles is the wider the smaller is the offset of the rotation angles from the calculated ones.

However, the manufacture of the delay line components with the exact sizes determined by system (10) is a time-consuming and not always feasible task. In real systems, the thicknesses of the components always differ from the calculated ones; at the same time, by varying the rotation angle of one component or the rotation angles of both components, it is possible to pick up a delay line configuration, wherein a thickness of at least one of the components is a solution of equations (10). Figure 3 also shows the adjustment curves of the composite delay line consisting of BK7 glass plates for the case when the thicknesses of the components do not satisfy the equations (10). Curve (*2*) corresponds to the case when the thickness of the second component of greater thickness is by 11.5 μm less compared to the optimal calculated thickness. Curve (*3*) reflects the case when the thickness of the second component exceeds by the same amount the calculated value, which corresponds to the measured thickness of the plate that has been used in the experiment. It should be clarified that curves (*2*) and (*3*) are constructed without taking into account the restrictions on the region of permissible rotations of the delay line components for the plates of nonoptimal thickness, which is substantially less than that shown in Fig. 3. The narrowing of that region is illustrated in Fig. 4, which shows the adjustment curve of the composite delay line consisting of BK7 glass plates manufactured for experimental testing (thickness h_1 = 610.3 μm and h_2 = 672.8 μm). The thickness h_2 of the thick plate exceeds that of the calculated one by more 11.5 μm, which makes optimal adjustment of the delay line impossible. In this case, the possibility of the delay line adjustment is considerably limited, as shown in the insets in Fig. 4, where the black colour indicates the regions of angles where the condition $\eta > 4$ is obeyed. The condition $\eta > 12$ is nowhere satisfied in the configuration in question, and the maximum possible suppression of the mirror artefact using these plates amounts to 10 dB. The required positioning accuracy of the thin plate is 10′, fine adjustment of the delay line is carried out by rotating the thick plate. The required adjustment accuracy of the thick plate is determined by the position of the thin plate and amounts to ~ 6′.

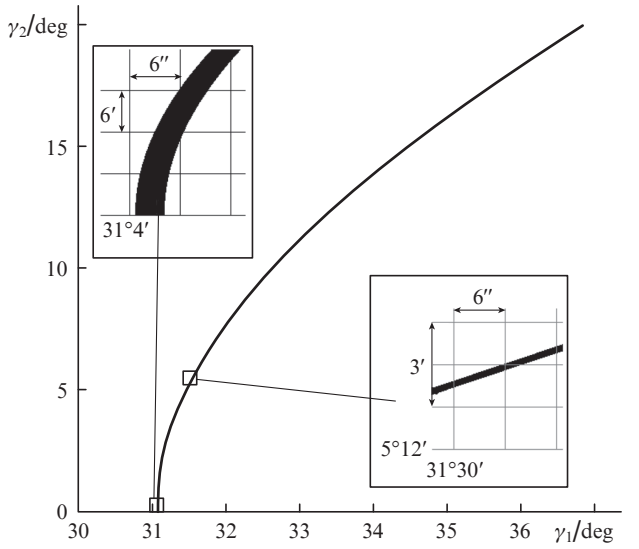

Figure 4. Adjustment curve of the composite delay line for the plates manufactured of BK7 glass and designated for experimental testing.

In the region of optimal rotation angles of a thin plate (for the experimental system γ_1 = 31°4′1″–31°4′4″) the accuracy requirements are somewhat lower, and the required accuracy to adjust the thick plate position is 24′.

3. Experimental testing of the possibility of simultaneous recording the quadrature spectral components

To experimentally demonstrate the possibility of simultaneous recording of quadrature spectral components of the back-

scatter signal, a laboratory setup based on the air Michelson interferometer was designed and manufactured.

The composite optical element separating the reference beam into two components with different delays was introduced into a standard optical circuit of the air Michelson interferometer. A superluminescent diode with the centre wavelength of 1040 nm and the spectral width at half maximum of 70 nm was used as a light source.

The phase-shifting element is made of BK7 glass plates with the measured thicknesses of $h_1 = 610.3$ μm and $h_1 = 672.8$ μm. The estimated angle between the plates is 31°.

The dispersive element of the spectrometer consists of a diffraction grating (LSFSG1000, LightSmyth, USA) and a prism that minimises the distortions caused by the nonlinearity of the frequency scale (nonequidistant spacing) in the process of registration of the optical spectral components [20]. As a focusing element, a home-made three-lens plan-objective (focal length 86 mm) with an external aperture diaphragm and minimal distortion (0.02% at the edge of the field of view) is used. The recording of intensity of spectral components is carried out by means of the linear CCD element SU-512LSB-DUAL (Goodrich, USA).

The task of experimental testing was to compare the efficiency of the use of the composite phase-shifting element and the simplest delay line, with no correction of its length, for different spectral components. In the most obvious case, such a delay line may be constructed as a stepped mirror with the step height equal to 1/8 of the centre wavelength of the light. The stepped delay line was proposed in [19] with the aim of improvement of the installation for the Michelson–Morley experiment. Later, the same line was implemented for registration of the quadrature components of radiation using the phase microscopy method (U.S. Patent S20070003436). However, the manufacture of such a mirror represents a separate and rather complicated problem because it requires the use of high-precision technological processes to ensure the deposition of a step of 130 nm height. Furthermore, such a mirror should have sufficiently large cross-sectional dimensions to ensure the possibility for neglect of the fringe effect at the step. This, in turn, in addition to the difficulties in manufacture, is in contradiction with the requirement of minimising the mass of the reference reflector, which is necessary for effective suppression of the coherent noise and is implemented in accordance with the procedure described in [21]. As an alternative to the use of the stepped mirror to compare the effectiveness of the air and achromatised delays, a sequential recording of the quadrature components on one and the same array of photocells was implemented. To this end, the position of the reference reflector between the neighbouring A-scans was changed on a discrete value [16] equal to 1/8 of the centre wavelength of the light source used. The distortions arising from the uniformity of scanning the probe beam across the object surface were eliminated according to the approach described in [22].

Figure 5 represents the experimentally recorded profiles of the scattered signal obtained for a low-reflectance mirror. Curve (*1*) corresponds to the profile registered in case of the optimum adjustment of the air delay line. In this case, the suppression of the mirror artefact peak is 33.3 dB. Curve (*2*) corresponds to the profile registered by means of a phase-shifting element. The suppression of the mirror artefact peak in this case amounts to 41.9 dB. Thus, the additional suppression of the mirror artefact peak in this experiment proves to be 9 dB, which is close to the theoretical estimates given above. The components of the phase-shifting element have been manufactured without the AR coatings, and so the signal values in the direct peak for curves (*1*) and (*2*) are slightly (by 0.1 dB) different. It should be noted that for the clarity and to enable a visual comparison of the effects observed in the analysis of the A-scans (Fig. 5) and two-dimensional images (Fig. 6), the noise amplitude is artificially reduced in Fig. 5, which is attained by averaging the images. This operation is justified, since in the observation of two-dimensional images, the brightness of which corresponds to the signal under restoration, the extended objects, the signals of which are comparable with the noise level, are well-distinguishable, whereas they are not detectable on the profile of the scattering signal. Two-dimensional images of the scattering surface positioned at an angle to the axis of the probe beam are presented in Fig. 6. The number 1 indicates the 'direct' images of this surface, and the number 2 corresponds to the artefact

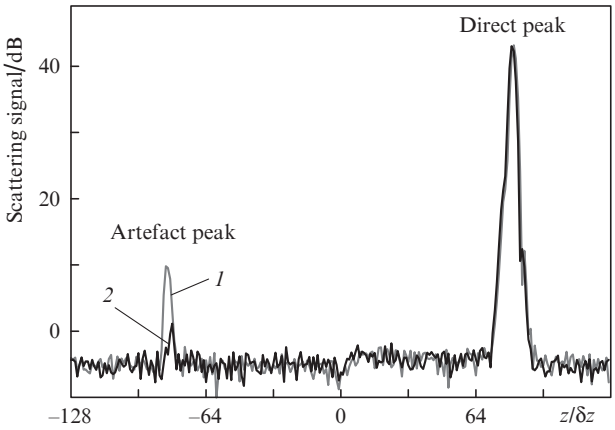

Figure 5. Restored A-scans with a small mirror reflectance when using the air delay line (*1*) and the phase-shifting element (*2*).

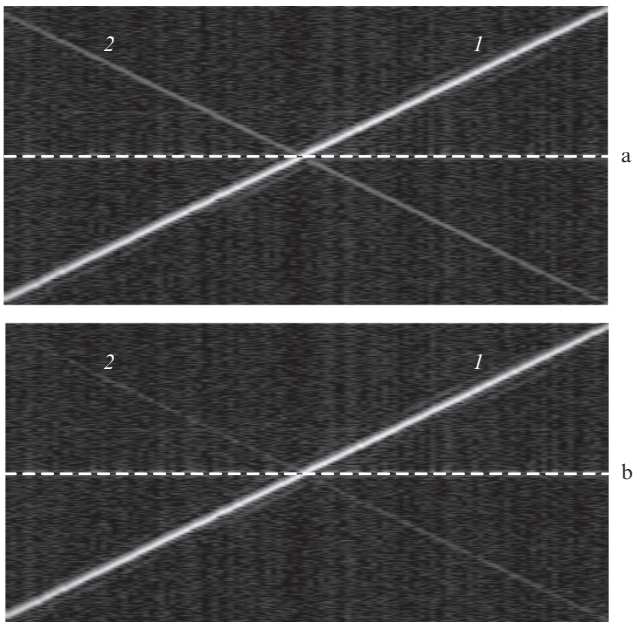

Figure 6. Images of the scattering surface positioned at an angle to the probe beam axis, by using (a) an inclined reflector and (b) the phase-shifting element.

images caused by the incomplete achromatism of the delay line. The dashed white line indicates the position of zero path difference of the reference and object waves. It is clearly seen that the artefact image is barely distinguishable against the background noise when the phase-shifting element is used, which means that the artefact image will not be observed in the study of the objects with a lower signal level typical for biological objects.

4. Conclusions

A new method for the simultaneous recording of the spectral components with the close-to-quadrature phase shift between two parts of the reference wave has been developed and experimentally tested. The phase-shifting element consists of a beam splitter that splits the reference optical beam into two beams and of the delay lines being individual for each beam, which create, in case of double-pass radiation, the mutual phase difference of $\pi/2$ close to achromatic. The achromatism of the phase shift over a wide spectral range is achieved by the use of the delay lines with different dispersion characteristics in the reference arm of the interferometer. By using such elements, we have proposed to employ the plane-parallel plates manufactured of the same material and placed in the optical system at different angles to the direction of the reference beam propagation.

The estimates of the ranges of admissible adjustment parameters for the achromatised delay lines carried out for the newly formulated criteria of efficient correction of the delay line dispersion indicate the possibility of practical implementation of the method proposed.

The suppression of the artefact mirror peak is experimentally achieved in the OCT-signal by an additional 9 dB compared to the level of its suppression when using the air delay line. The two-dimensional images of the plane boundary between the two media, positioned at an angle to the axis of the probe beam, are obtained by means of the mirror artefact correction with maintaining the dynamic range.

Acknowledgements. This work was partially supported by the Russian Foundation for Basic Research (Grant No. 12-02-31754) and the Government of the Russian Federation (Grant No. 14.B25.31.0015).

References

1. Fercher A.F., Roth E. *Proc. SPIE Int. Soc. Opt. Eng.*, **0658**, 4851 (1986).
2. Fercher A.F., Mengedoht K., Werner W. *Opt. Lett.*, **13**, 186 (1988).
3. Zimnyakov D.A., Tuchin V.V. *Kvantovaya Elektron.*, **32**, 849 (2002) [*Quantum Electron.*, **32**, 849 (2002)].
4. Fercher A.F., Hitzenberger C.K., Kamp G., Elzaiat S.Y. *Opt. Commun.*, **117**, 43 (1995).
5. Fercher A.F. *J. Biomed. Opt.*, **1**, 157 (1996).
6. Choma M.A., Sarunic M.V., Yang C.H., Izatt J.A. *Opt. Express*, **11**, 2183 (2003).
7. Hu Z., Rollins A.M. *Opt. Lett.*, **32**, 3525 (2007).
8. Fercher A.F., Leitgeb R.A., Hitzenberger C.K., Sattmann H., Wojtkowski M. *Proc. SPIE Int. Soc. Opt. Eng.*, **3564**, 173176 (1999).
9. Wang R.K. *Appl. Phys. Lett.*, **90**, 054103 (2007).
10. An L., Wang R.K. *Opt. Lett.*, **32**, 3423 (2007).
11. Wojtkowski M., Kowalczyk A., Leitgeb R., Fercher A.F. *Opt. Lett.*, **27**, 1415 (2002).
12. Leitgeb R.A., Hitzenberger C.K., Fercher A.F., Bajraszewski T. *Opt. Lett.*, **28**, 2201 (2003).
13. Targowski P., Wojtkowski M., Kowalczyk A., Bajraszewski T., Szkulmowski M., Gorczynska W. *Opt. Commun.*, **229**, 79 (2004).
14. Gelikonov V.M., Kasatkina I.V., Shilyagin P.A. *Izv. Vyssh. Uchebn. Zaved., Ser. Radiof.*, **52**, 897 (2009) [*Radiophys. Quantum Electron.*, **52**, 810 (2009)].
15. Bachmann A.H., Leitgeb R.A., Lasser T. *Opt. Express*, **14**, 1487 (2006).
16. Leitgeb R.A., Wojtkowski M., in *Optical Coherence Tomography: Techology and Applications* (Berlin: Springer, 2008) p. 177.
17. Choma M.A., Yang C.H., Izatt J.A. *Opt. Lett.*, **28**, 2162 (2003).
18. Gelikonov G.V., Gelikonov V.M., Moiseev A.A., Shilyagin P.A. *Proc. SPIE Int. Soc. Opt. Eng.*, **8213**, 82133L (2012).
19. Kennedy R.J. *Proc. Nat. Acad. Sci. USA*, **12**, 621 (1926).
20. Gelikonov V.M., Gelikonov G.V., Shilyagin P.A. *Opt. Spektrosk.*, **106**, 518 (2009) [*Opt. Spectrosc.*, **106**, 459 (2009)].
21. Gelikonov V.M., Gelikonov G.V., Kasatkina I.V., Terpelov D.A., Shilyagin P.A. *Opt. Spektrosk.*, **106**, 1006 (2009) [*Opt. Spectrosc.*, **106**, 895 (2009)].
22. Gelikonov V.M., Gelikonov G.V., Terpelov D.A., Shabanov D.V., Shilyagin P.A. *Kvantovaya Elektron.*, **42**, 390 (2012) [*Quantum Electron.*, **42**, 390 (2012)].